

SphinX: The *Solar Photometer in X-Rays*

Szymon Gburek · Janusz Sylwester · Miroslaw Kowalinski · Jaroslaw Bakala ·
Zbigniew Kordylewski · Piotr Podgorski · Stefan Plocieniak · Marek Siarkowski ·
Barbara Sylwester · Witold Trzebinski · Sergey V. Kuzin · Andrey A. Pertsov ·
Yuriy D. Kotov · Frantisek Farnik · Fabio Reale · Kenneth J.H. Phillips

Received: 10 April 2012 / Accepted: 19 November 2012 / Published online: 13 December 2012
© Springer Science+Business Media Dordrecht 2012

Abstract *Solar Photometer in X-rays* (SphinX) was a spectrophotometer developed to observe the Sun in soft X-rays. The instrument observed in the energy range $\approx 1\text{--}15$ keV with resolution ≈ 0.4 keV. SphinX was flown on the Russian CORONAS–PHOTON satellite placed inside the TESIS EUV and X telescope assembly. The spacecraft launch took place on 30 January 2009 at 13:30 UT at the Plesetsk Cosmodrome in Russia. The SphinX experiment mission began a couple of weeks later on 20 February 2009 when the first telemetry dumps were received. The mission ended nine months later on 29 November 2009 when data transmission was terminated. SphinX provided an excellent set of observations during very low solar activity. This was indeed the period in which solar activity dropped to the lowest level observed in X-rays ever. The SphinX instrument design, construction, and operation principle are described. Information on SphinX data repositories, dissemination methods, format, and calibration is given together with general recommendations for data users. Scientific research areas in which SphinX data find application are reviewed.

S. Gburek (✉) · J. Sylwester · M. Kowalinski · J. Bakala · Z. Kordylewski · P. Podgorski ·
S. Plocieniak · M. Siarkowski · B. Sylwester · W. Trzebinski
Space Research Center, Polish Academy of Sciences, Wrocław, Poland
e-mail: sg@cbk.pan.wroc.pl

S.V. Kuzin · A.A. Pertsov
Lebedev Physical Institute of the Russian Academy of Sciences, Moscow, Russia

Y.D. Kotov
National Research Nuclear University “MEPhI”, Moscow, Russia

F. Farnik
Astronomical Institute of Academy of Sciences of the Czech Republic, Ondřejov, Czech Republic

F. Reale
INAF, G.S. Vaiana Astronomical Observatory, Palermo, Italy

K.J.H. Phillips
Mullard Space Science Laboratory, University College London, Holmbury St Mary, Dorking, Surrey,
UK

Keywords Solar corona · Solar instrumentation · X-rays

1. Introduction

Investigations and monitoring of solar soft X-ray flux in the energy range $\approx 1.0\text{--}15.0$ keV play a crucial role in exploring the physics of the solar corona, determining plasma-diagnostics parameters, research on coronal-heating mechanisms, physics of flares, space weather, and climate. The key idea behind the SphinX project development was to deliver a fast spectrometer that could provide good quality measurements of soft X-ray flux over its entire variability range, which extends over seven orders of magnitude. This was achieved by the use of three detectors with decreasing effective areas in the main SphinX X-ray measurement assembly. Pure silicon PIN diodes of the type XR-100CR produced by US Amptek Inc. were chosen as SphinX X-ray detectors. These diodes had already been used in space on the *Solar X-ray Spectrometer* (SOXS) instrument (Jain *et al.*, 2005) before the SphinX flight.

SphinX flew on the Russian CORONAS-PHOTON satellite (Kotov, 2011). It was the third satellite launched in the Russian *Complex Orbital Observations Near-Earth of Activity of the Sun* (CORONAS) program. SphinX operated in orbit within the TESIS EUV and X telescope assembly developed at the P.N. Lebedev Physical Institute (LPI) and described by Kuzin *et al.* (2011). The spacecraft was launched on 30 January 2009 at 13:30 UT from the Plesetsk Cosmodrome in northern Russia.

The spacecraft orbit was circular with an inclination angle of 82.5° , initial height 550 km, and period of 95 minutes. The accuracy of the spacecraft orientation with respect to the Sun was better than three arcminutes after stabilization.

The effective areas of the detectors were chosen so that SphinX was capable of measuring the flux at the level 100 times below the detection threshold of the X-Ray Sensors (Hanser and Sellers, 1996; Bornmann *et al.*, 1996; Reinard *et al.*, 2005) of the *Geosynchronous Operational Environmental Satellite* (GOES) which operates in a geosynchronous orbit, $\approx 36\,000$ km above the surface of the Earth.

The upper limit for the solar X-ray flux values that could be measured correctly by SphinX was high enough to observe the strongest flares for which GOES detectors become saturated near event peak phase.

Special care was taken during SphinX development in order to improve the spectral purity of the instrument measurements. Construction elements were placed in such a way that fluorescence excited by solar X-rays could not reach the detector entrance windows. Detectors selected by the SphinX team were equipped with additional internal collimator that also reduced the level of spurious illumination of the detector silicon crystals. The SphinX operation principle was chosen so that it was not necessary to use additional attenuators to prevent detector saturation. Attenuators also could be a source of fluorescence contamination in observed fluxes as is known from analysis of the *Reuven Ramaty High Energy Solar Spectroscopic Imager* (RHESSI) data (Lin *et al.*, 2002). RHESSI was launched on 5 February 2002 and is still operating in a nearly circular orbit, with inclination angle of 38° and altitude of 600 km. This instrument uses germanium detectors to measure soft and hard solar X-rays. The RHESSI effective area is very small below 6 keV. Thus SphinX measurements can be useful in calibration of RHESSI data in the energy range $\approx 1\text{--}6$ keV recorded in 2009.

Due to the large volume of RHESSI detectors, a substantial orbital background is seen in the data particularly during low solar-activity periods. This background hinders event identification and makes it difficult to determine actual X-ray flux level. The SphinX detectors

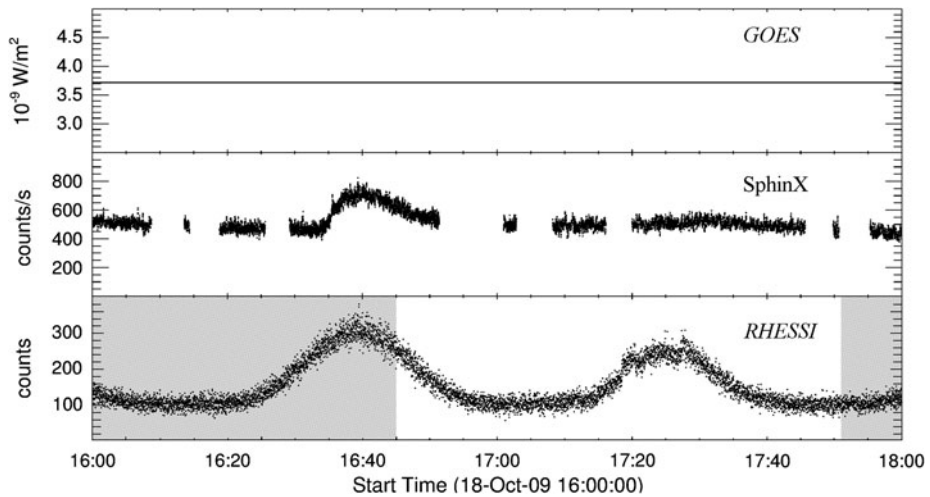


Figure 1 Comparison of solar X-ray observations on 18 October 2009. Top: the GOES light curve in $1-8 \text{ \AA}$ ($1.5-12.4 \text{ keV}$) channel; SphinX light curve in the same energy range as for GOES is plotted in the middle panel. The RHESSI light curve in ($3.0-12.4 \text{ keV}$) range is shown at the bottom. Shaded areas in this plot are for intervals of time when RHESSI was eclipsed. The GOES curve is entirely flat and follows the instrument sensitivity threshold, $3.7 \times 10^{-9} \text{ W m}^{-2}$. Substantial modulation from the orbital background is seen in the RHESSI light curve. Due to the satellite night, the RHESSI also missed a small flaring event, which is seen in the SphinX light curve.

were much smaller than the RHESSI ones and therefore less sensitive to particle hits. Thus a strong orbital background was seen in SphinX measurements only during spacecraft passages through radiation belts and the South Atlantic Anomaly (SAA). Outside the SAA and the radiation belts, the orbital-background contribution is small in the SphinX data. Various factors, such as spacecraft nights, lack of sensitivity, and orbital background, are such that sometimes SphinX data are only available for spectrophotometric analysis in the soft X-rays. An example is shown in Figure 1.

The instrument was developed entirely in Wrocław by the Solar Physics Division Team of the Space Research Centre Polish Academy of Sciences (SRC-PAS) in a very short time. First work on SphinX construction started three years before launch.

SphinX data are available from 20 February until 29 November 2009 with almost continuous coverage. The SphinX mission had two phases. The first phase lasted from 20 February until 6 April 2009. This phase was used by the SphinX team to find an optimum data-acquisition strategy. SphinX on-board software changes took place during the first mission phase. The optimum SphinX operation strategy was found and fixed on 6 April 2009. From that time no further changes in the software were made until the end of the mission. The instrument sent compressed data to satellite telemetry systems with a rate of $\approx 150 \text{ Mb day}^{-1}$.

The scientific objectives assumed during the experiment development were as follows:

- Studies of heating processes in quiet solar corona using analysis of photon arrival time.
- Solar soft X-ray radiation monitoring over seven orders of magnitude in intensity.
- Determination of physical parameters (T , EM, DEM) of solar coronal plasma and analysis of their variability in time.
- Identification of transient ionization effects in solar plasma in order to determine densities of flaring plasma.
- Analysis of solar soft X-ray flux oscillations with period in the $1-500$ seconds range.

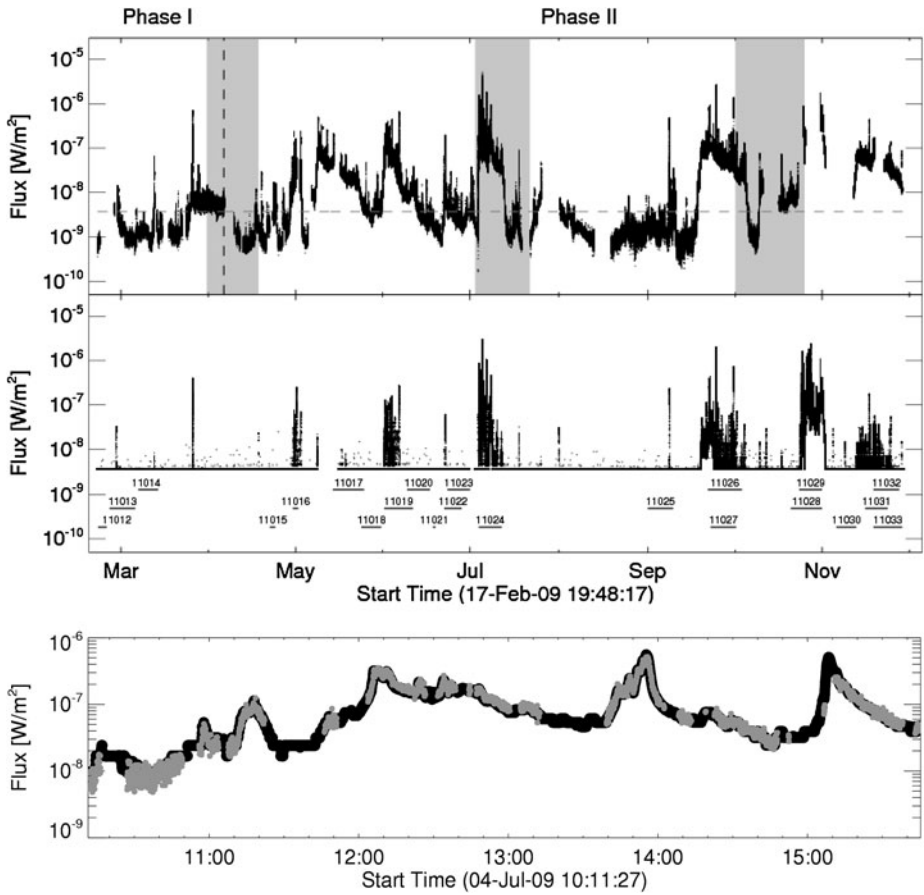


Figure 2 The SphinX light curve over the mission duration is shown in the upper panel. The black dashed vertical line is for 6 April 2009, when the first mission phase ended and the second began. The horizontal gray dashed line shows the GOES sensitivity detection threshold ($3.7 \times 10^{-9} \text{ W m}^{-2}$). Gray vertical strips show the time intervals when satellite nights did not occur – the long spacecraft days. The GOES light curve is shown in the middle panel for comparison. Active-region lifetimes are indicated by gray intervals there. Numbers of the active regions as attributed by the National Oceanic and Atmospheric Administration (NOAA) are given above. The bottom panel shows a comparison of SphinX (gray curve) and GOES (black curve) fluxes in the 1–8 Å wavelength range for a shorter time period. Gaps in SphinX data occur for temporal intervals when the detectors were exposed to energetic particles.

- Analysis plasma chemical composition and abundance variability in solar corona for elements: Al, Ar, Ca, Fe, Mg, Si, and S.
- Verification of the novel, fluorescence-based, photometry measurement method.
- Development of a reference photometric standard in soft X-rays with an absolute accuracy of 10 %.

SphinX observed the Sun in soft X-rays during a period of a very low solar activity between Cycle 23 and 24 and in the Cycle 24 early rise phase. The overview of SphinX observations is shown in Figure 2. The bottom plot of this figure shows that SphinX and GOES observed fluxes demonstrating comparable behavior in the 1–8 Å wavelength range. The discrepancies between SphinX and GOES flux values are on average 10 % for the tem-

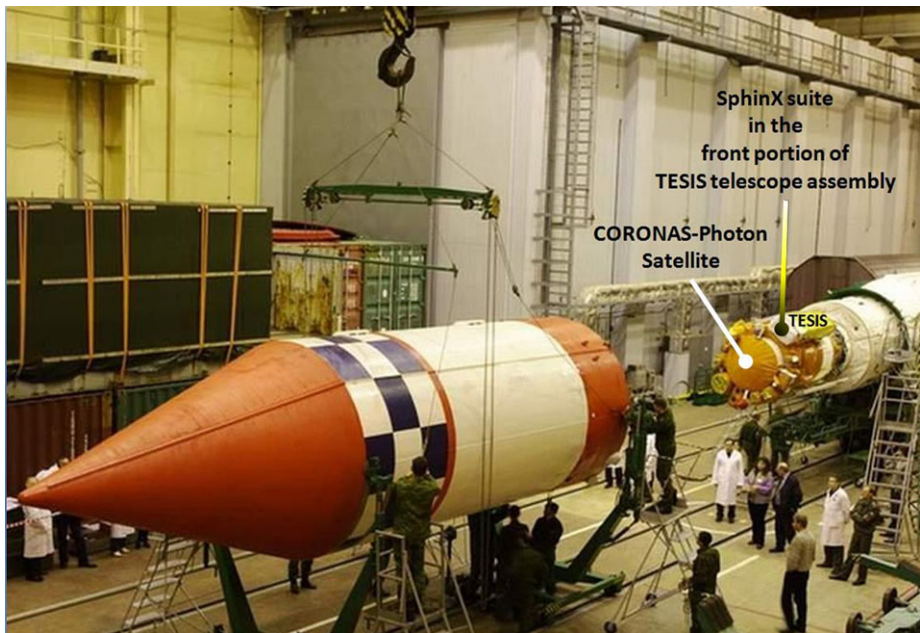


Figure 3 Integration of the CORONAS–PHOTON satellite with the Cyclone-3M buster. Locations of SphinX and TESIS are indicated in the picture.

poral interval shown in the plot. Further improvements in cross-calibrations of SphinX and GOES measurements may be achieved by thorough studies of both instruments' responses and housekeeping data.

Due to very low solar flux during the mission, some objectives assumed during instrument construction were not achieved and some reached only partly. The first descriptions of SphinX can be found in Sylwester *et al.* (2008), Gburek *et al.* (2011a, 2011b). The focus of this work is on describing what was the actual output of the experiment and identifying fields of applications for the collected dataset. A description of the instrument's construction, its mission, calibration, and data is also given.

2. The Satellite and Orbit Environment

The main objective of the CORONAS–PHOTON mission was the study of the solar electromagnetic radiation in a broad energy interval ranging from UV to γ -radiation of energies up to ≈ 2000 MeV.

CORONAS–PHOTON was a multi-experiment satellite for which instruments were constructed and provided by Russian, Indian, Ukrainian, and Polish partners. The nominal mission lifetime was expected to be at least three years but it ended about ten months after launch due to technical problems with the satellite.

The spacecraft weighted about two tons and was launched by a Cyclone-3M rocket. The launcher and the satellite are shown in Figure 3.

In the CORONAS–PHOTON orbit, periods occurred in which spacecraft was hidden behind the Earth and did not see the Sun. These nights lasted up to about half an hour. On the other hand there were periods in which nights did not occur and the satellite saw the Sun

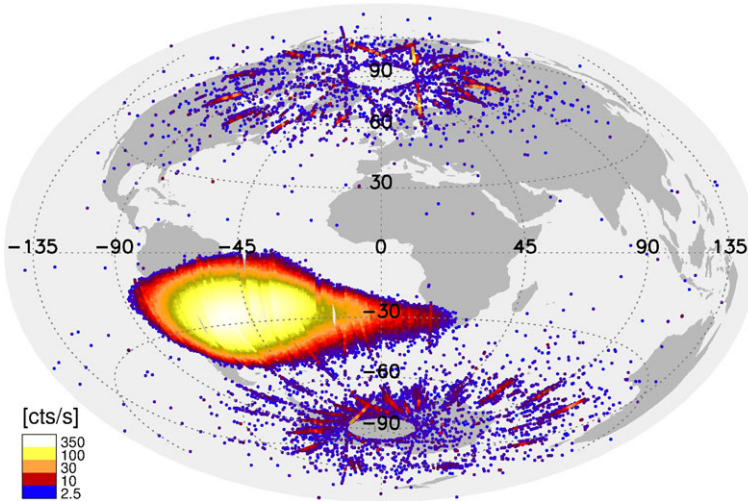


Figure 4 Energetic-particle distribution over CORONAS-PHOTON orbit as observed by SphinX. It is seen that particles contribute to measurement everywhere on the orbit. This contribution is small in equatorial regions. It increases substantially in radiation belts and becomes particularly strong in the SAA area.

without interruptions. These long days lasted for two–three weeks. There were three long orbital days during the CORONAS-PHOTON mission in April, July, and October 2009.

The high inclination angle of the orbit was such that the satellite had to cross radiation belts and the SAA during the flight. In these regions the energetic particles increased, which caused a strong additional background to appear in the data from the instruments. The particle contribution to the measurements needs to be investigated in detail in order to determine the background level, which is important for data-analysis purposes. Particle signal measurements also allow for interesting studies of their distribution at the satellite orbit. An example of the energetic-particle environment distribution is shown in Figure 4.

3. SphinX Construction

SphinX was a rather compact instrument. All of the detectors, electronic boards, and other elements were placed in an aluminum housing of $27 \times 28 \times 8$ cm. The instrument's mass was about ≈ 3.7 kg and peak power consumption 10 W. The detectors were fixed to a copper support plate from which heat was transferred to a satellite radiator by a sink pipe. The detector support plate was thermally isolated from the rest of the instrument. The active-cooling system allowed the detector crystal temperature to be maintained about 50°C below the support plate temperature. The SphinX flight unit is shown in Figure 5. Construction details are revealed in the instrument's CAD exploded plots in Figure 6.

Construction of SphinX was accomplished in 2007. Next a series of tests were performed in order to check if the flight unit could be launched safely and survive the harsh orbital environment. First tests took place in Warsaw in a thermal-vacuum chamber. These tests proved that SphinX can operate correctly in vacuum and the expected temperature range on orbit. Then mechanical, acoustic, and vibration tests were done in Prague to check if SphinX was mechanically robust enough to survive launch. After the endurance tests, X-ray calibrations of the instrument were performed in Palermo and Berlin. These tests were and

Figure 5 A photograph of the SphinX flight unit. The SphinX box sizes were 28 cm length, 27 cm height, and 8 cm width.



are important for reduction and analysis of data recorded during the mission. We give an extended description of the SphinX calibration tests below.

4. SphinX Detectors and Principles of Operation

For soft X-ray measurements, SphinX was equipped with four XR-100CR detectors provided by Amptek Inc., Bedford, MA, USA. These detectors were 500 μm thick, pure silicon PIN diodes with entrance windows covered with 12.7 μm thick beryllium foil. Each detector also had a temperature sensor, Peltier cooler, and FET transistor inside the package. One of the SphinX detectors and some details of its construction are shown in Figure 7. SphinX detectors were operated in flight at temperatures below $-20\text{ }^{\circ}\text{C}$.

During SphinX development we planned to observe the solar X-ray flux in its entire dynamic range, which covers seven orders of magnitude. A single XR-100CR detector can measure correctly only low-level solar X-ray fluxes and would saturate even at moderate-flux events. Thus a dedicated assembly consisting of three detectors was constructed for solar X-ray measurements. The main idea behind that assembly design was to use extra apertures in front of the detectors and limit their sensitivity to X-ray flux this way.

Eventually the SphinX X-ray detector assembly came up with one detector (D1) of entrance aperture 21.50 mm^2 (the nominal factory entrance-window area), the second one (D2) with aperture of 0.495 mm^2 for measuring moderate X-ray fluxes, and the third (D3) with aperture of 0.01008 mm^2 for measurements of strong flux.

SphinX also had one XR-100CR detector in a separate and independent fluorescence-measurement block. The block was designed to measure fluorescence radiation excited by solar X-rays on selected pure target foils. The SphinX fluorescence block necessitated stronger solar X-ray flux (above GOES class M1) to operate properly and was never switched on, due to very low activity of the Sun during the SphinX mission. More details regarding the SphinX fluorescence block are given by Gburek *et al.* (2011b).

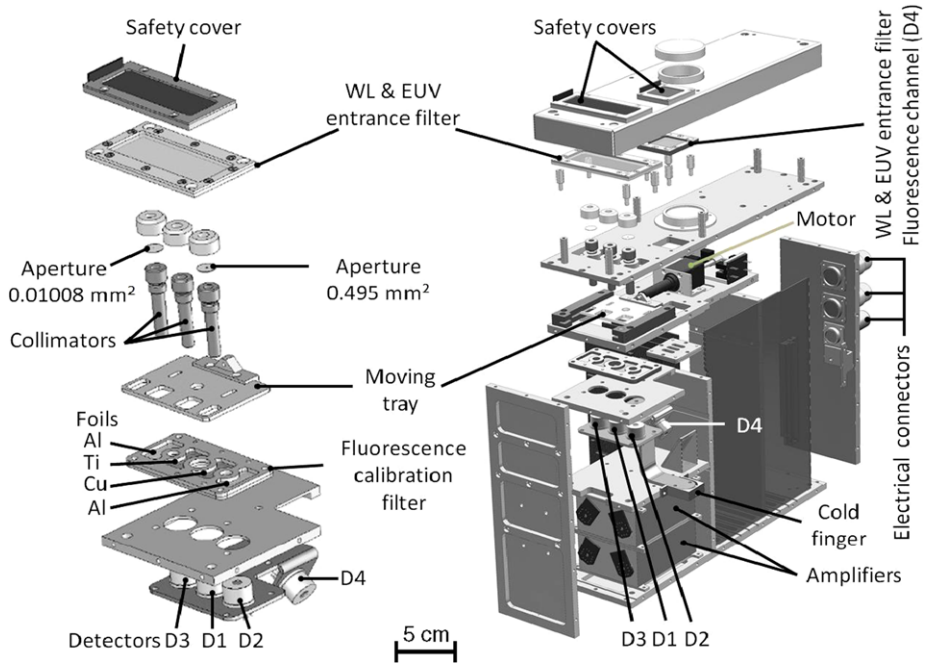
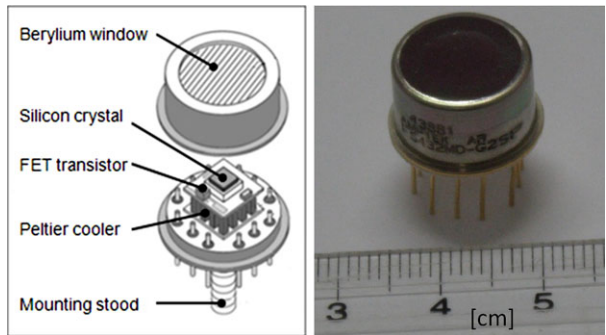


Figure 6 SphinX CAD exploded plots. The X-ray optical bench of the instrument is shown in more detail at the left.

Figure 7 Amptek XR-100CR detector used in SphinX.



A moveable element in SphinX was a shutter with a set of openings. The shutter could be moved by a linear actuator and would be used to cut off X-ray illumination and in this way protect the two more sensitive detectors D1 and D2 if a large event happened.

The shutter could also be moved to a calibration position in which all of the detectors would not receive direct solar X-rays but would be exposed to a fluorescence illumination coming from foils in a calibration filter placed over the detectors (the position of the fluorescence calibration filter is shown in Figure 6). In this calibration operation mode, SphinX detectors would simultaneously receive characteristic radiation from aluminum ($K\alpha$ at 1.49 keV), titanium ($K\alpha$ at 4.51 keV), and copper ($K\alpha$ at 8.05 keV) foils. Thus spectra collected during in-flight calibration sessions would have three peaks, well separated in energy. Positions of the peaks together with their amplitudes could be used to perform actual

Table 1 SphinX detector measurement channel parameters.

X-ray flux level	Low	Moderate	High	High
Detector Name	D1	D2	D3	D4
Observation type	Direct Solar X-rays	Direct Solar X-rays	Direct Solar X-rays	Fluorescence
Aperture [mm ²]	21.500 ^A	0.4947 ^S	0.01008 ^S	11.1 ^A
Energy FWHM [eV]	480 ^B	350 ^B	370 ^B	290 ^P
Pulse width [μ s]	1.25 ^E	4.17 ^E	4.17 ^E	4.17 ^E
Energy range [keV]	1.0–15	0.85–15	0.85–15	0.85–15

A: based on Amptek technical drawings of respective detector, S: measured at SRC–PAS Wroclaw under microscope, B: based on BESSY measurements, P: based on Palermo X-ray calibrations. E: measured at SRC–PAS using oscilloscope.

instrument energy calibrations, control pile-up effects, and give information on sensitivity changes. To obtain a good signal-to-noise ratio in the spectra during calibration mode, SphinX needed stronger X-ray fluxes (minimum of GOES M1 level). Such flux values were not available during the SphinX mission. Thus the calibration mode was never switched on. A more extended description of the SphinX in-flight calibration capabilities can be found in Gburek *et al.* (2011b).

Due to the very low activity of the Sun in the period of SphinX in-orbit operation, there are no useful data from the least sensitive detector in the SphinX main X-ray detector assembly. It detected only noise. There is some useful signal above the noise in data recorded by the detector, which was meant to be operated at moderate solar X-ray flux level, but these measurements are always accompanied by simultaneous measurements from the most sensitive SphinX detector with much better statistics. Thus, in what follows, we focus mainly on data recorded by the detector with the largest effective area, which are the best for purposes of scientific data analysis.

5. SphinX Data Format, Access, and Calibration Information

Each SphinX measurement channel consisted of a detector connected to an amplifier–shaper system whose output was read by an analog-to-digital converter and sent to an on-board computer. On orbit, SphinX measured in spectral mode and event-counting mode. In the event-counting mode, every single pulse that appeared at the amplifier–shaper output was processed and information on the pulse amplitude and time of occurrence stored in memory. The pulse amplitude was converted to a channel number in the spectrometer’s 256 channel space. This measurement method is known as pulse of height analysis (PHA). Studies on SphinX calibration data showed that 256 is an optimum number of energy channels for SphinX operations in flight. Thus, all SphinX multichannel analyzers had 256 energy channels covering the nominal energy range 0.0–15.0 keV. The useful energy ranges depend on the particular measurement channel sensitivity. They are given in Table 1.

Individual pulse-arrival times were determined with 1 μ s accuracy. The system could distinguish and correctly measure amplitudes of two pulses occurring $\approx 6 \mu$ s one after another. If the time delay between two successive pulses was less than $\approx 6 \mu$ s, they started to blend and the electronics measured higher amplitude than the amplitudes of the contributing pulses. This caused a pile-up effect in the data.

The pulses had different origins. They were produced on the output of the amplifier–shaper when an X-ray photon hit the detector crystal. The pulse amplitude was proportional

to the photon energy in these cases. Pulses were also produced when energetic particles hit the detector's sensitive volume. In such a case, the recorded pulse amplitude had no obvious physical interpretation. Another source of pulses was the measurement channel electronics itself. It had to be reset every couple of seconds. After resets, additional pulses were produced at the amplifier–shaper output. Many particle and reset-originating pulses had a large amplitude and thus are seen in the last SphinX energy channel (bin 256), which allows one to identify them.

Information on SphinX detected events, represented by a pair, consisting of energy channel number (one byte) and arrival time (three bytes), were stored by the SphinX on-board computer in memory frames 8 kB in size. A single frame could store information for more than 1000 events.

In the spectral observing mode, SphinX provided information on the total number of events to which channel number was attributed in a selected range in the instrument bin space. These histograms and their total collection times (the spectrum exposures) were stored together with the events in the same eight kB telemetry frames. During the mission, SphinX recorded only 256-channel and ancillary broadband, 4-channel spectra (so-called basic mode spectra).

The first channel of the basic mode spectra contains mainly electronic noise. In the second and third channels solar X-ray flux was recorded in the energy ranges 1.5–3.0 keV and 3.0–14.9 keV for the D1 detector and 1.0–3.0 keV and 3.0–14.9 keV for the other detectors. The last channel of the basic mode contains the events caused by energetic particles and the instrument resets.

The event-counting operation mode is the most versatile one. All spectral-mode observations can be reconstructed from the event data. The spectral mode was mainly used by the SphinX on-board computer in order to quickly calculate flux rates. Thus the computer was capable of operating the instrument in different ways, depending on the actual flux level.

In addition to spectra and events, a housekeeping block of technical data was added to each memory frame. The frames were next compressed by the on-board computer and sent to telemetry. Usually, frames with SphinX data were processed with a cadence of one second. It was sometimes necessary to increase the frame processing time to five or eight seconds when spacecraft telemetry was heavily loaded.

The telemetry data from the spacecraft were received by a ground station in Moscow and then were sent through the internet to SRC–PAS. After decompression and reformatting, the telemetry data were stored in binary files. A single SphinX data file typically covers a couple of hours of the observing time and contains several thousand telemetry frames.

Binary files with SphinX raw data were successively reduced to level-0 format. Reduction started when the first telemetry dumps were received. The level-0 data files are written in the Interactive Data Language (IDL) native format. Spectra and event-counting observations are stored in these files as arrays. SphinX level-0 data can be used for the scientific analysis. Good knowledge of instrumental effects is necessary for this purpose, however. The internet catalogue with SphinX level-0 data, legend, and format description is available for public use (see the [Appendix](#), where links are given).

Conversion of SphinX level-0 data to the scientific-grade level-1 format took place in 2010. All data from the second mission phase were reduced to level-1 format. This data format is recommended for external users. Analysis and interpretation of level-1 data can be used without detailed knowledge of the instrumental effects. For the first mission phase the reduction to level-1 could not have been automated because of the many changes in instrument operation and on-board software performed during that time. SphinX level-1 data for the first mission phase will be made available in 2012 through the SphinX level-1 data catalogue, described below.

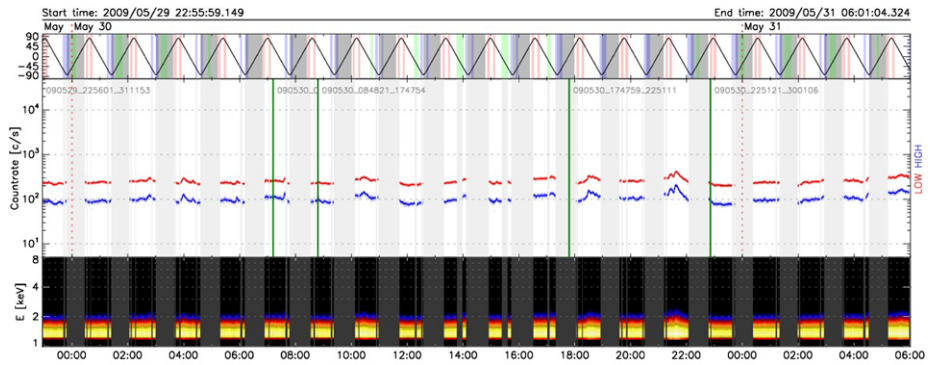


Figure 8 SphinX level-1 catalogue with visualization of the instrument measurements for 30 May 2009. The plotted time range is extended a bit to the previous and the next day. Spacecraft orbit latitude is shown in the top panel. In the middle panel two SphinX count rates are plotted. The red one is for the energy range 1.2–1.5 keV and the blue one for 1.5–15.0 keV range. Bottom panel: a dynamic spectrum of SphinX. Grayed areas indicate when there are no good quality measurements. These intervals occurred mainly during passages through the SAA, radiation belts, or spacecraft nights.

On-line public access to SphinX level-1 data is provided in the form of an internet catalogue a dedicated SphinX server (see the [Appendix](#) for the level-1 data catalogue links). The catalogue website is organized in the form of a calendar in which day fields link to SphinX daily summary pages with visualization of SphinX data and links for downloading level-1 data files. An example of a plot with visualization of SphinX data from the level-1 catalogue is shown in [Figure 8](#).

SphinX level-1 data are available as event lists in Flexible Image Transport System (FITS) files. The Office of Guest Investigator Programs (OGIP) FITS format was selected for SphinX level-1 data. This format is well standardized and documented. Information on the OGIP FITS format also can be accessed on the SphinX level-1 catalogue site.

All kinds of SphinX recorded events (caused by X-ray photons, particles, resets) are in the level-1 FITS files. A flag is attributed to each particular event with information on its origin. The flag allows us to filter events according to user-specified queries. For example users can filter out events of X-ray photon origin. Higher-level data products (light curves, spectra) can then be constructed from a filtered event set and used for X-ray spectral analysis. All of the necessary calibration information for scientific analysis of the instrument flight data is available in a SphinX response file. This file is also written in the OGIP FITS format. It contains the SphinX Detector Response Matrix (DRM) extension and another extension with energy edges for SphinX channels.

The SphinX level-1 catalogue has a legend and provides access to:

- description of SphinX level-1 data and their format,
- guide for SphinX users,
- IDL routines for processing SphinX level-1 data,
- example IDL programs developed at SRC–PAS for SphinX data processing,
- example level-1 FITS files and the calibration FITS with SphinX DRM,
- a description of the SphinX flag system.

Links to the above mentioned documents, software, and data are given in the [Appendix](#).

6. Sphinx Calibrations in X-Rays

Extensive X-ray calibration was performed before the Sphinx flight. The first Sphinx calibrations were performed in Palermo at the X-ray Astronomy Calibration and Testing (XACT) Facility (see the [Appendix](#) for a link to the XACT WWW site) in October 2007 (Collura *et al.*, 2008).

The facility is equipped with a 35-meter long stainless-steel tube with a large vacuum chamber (in which Sphinx was kept during tests) attached to one end and an X-ray source connected to the other end. The source used for Sphinx calibration produced X-rays by stopping accelerated electrons in the anode material. Thus the measured spectra mainly consisted of bremsstrahlung continuum with $K\alpha$ and $K\beta$ lines of the anode material superimposed. These spectra were measured simultaneously by Sphinx and two other calibrated spectrometers: one equipped with a gas-flow proportional counter and the second with a solid-state detector, similar to those used in Sphinx. Analysis of the spectra recorded by Sphinx allowed us to cross-calibrate the instrument channels in energy and to determine the energy resolution. By comparison of Sphinx and the XACT calibrated spectrometers measurements, it was also possible to estimate the Sphinx efficiency.

Final X-ray calibrations of Sphinx were performed at the Physikalisch-Technische Bundesanstalt (PTB) calibration facility using the BESSY II synchrotron as a primary source standard. PTB is the German National Metrology Institute. It is responsible for realization and dissemination of the legal standards in Germany (Klein, Thornagel, and Ulm, 2004).

During calibrations at BESSY II, Sphinx operated in a vacuum chamber connected to a metrology-class beamline. Thus it was possible to precisely determine all of the parameters necessary to calculate the actual flux received by the detectors. The Sphinx calibrations at BESSY II consisted of two separate experiments.

The first one was performed at a four-crystal monochromator (FCM) beamline. This beamline provides radiation in the form of a very narrow line centered at a given energy. The energy of the line is tunable over a broad spectral range. Beamline radiation has a high spectral purity and good reproducibility of the absolute photon flux. The flux strength of this monochromatic radiation can also be tuned over a broad range.

The use of the FCM beamline allowed one to light up the Sphinx detectors in selected energy lines. Analysis of data from these measurements provided information regarding the instrumental resolution curve shape. It was possible to determine pile-up-effect contributions to Sphinx observations using FCM beamline data. The FCM measurements also allowed us to scale the instrument channel. An example of data recorded by Sphinx at FCM beamline is shown in [Figure 9](#).

After completion of the measurements on the FCM beamline, the vacuum chamber with Sphinx was connected to another beamline where it was possible to expose detectors to undispersed synchrotron radiation. The spectra of such radiation can be calculated with a very high accuracy. These calculated BESSY II spectra were next compared ([Figure 10](#)) with the spectra measured by Sphinx to determine the instrument's sensitivity over the entire measurement energy range.

All of the calibration information provided by analysis of data collected during the Palermo and Berlin experiments was incorporated into the Sphinx DRMs.

Sphinx calibration experiments also allowed us to determine errors in the measurements. For data with good count statistics, when Poisson noise can be neglected, the measurement accuracy was at the level of $\approx 1\%$.

The calibration tests also revealed that the dark current for the Sphinx detectors can be neglected, provided that the detectors are operated below $-20\text{ }^{\circ}\text{C}$.

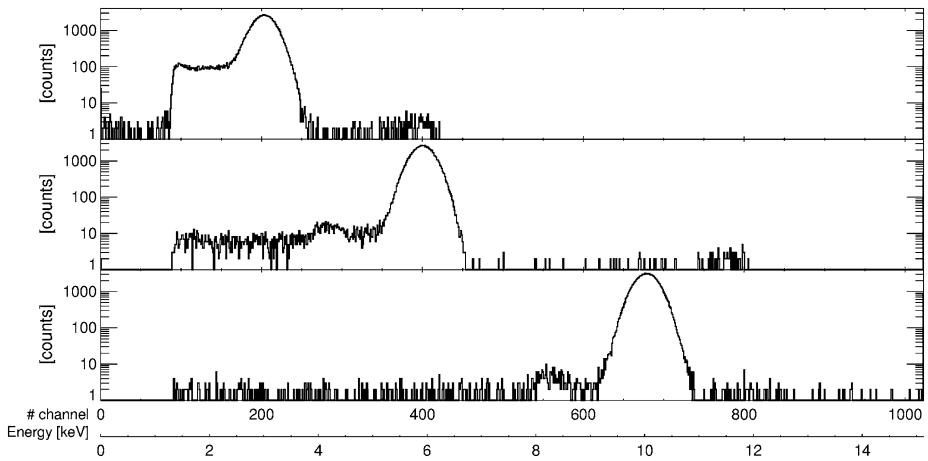


Figure 9 SphinX spectra recorded on FCM beamline for energies 3 keV (top panel), 5.9 keV (middle panel), and 10 keV (bottom panel). Escape peaks together with a shelf coming from partial charge collection are seen to the left of the main peaks, which are nearly Gaussian in shape.

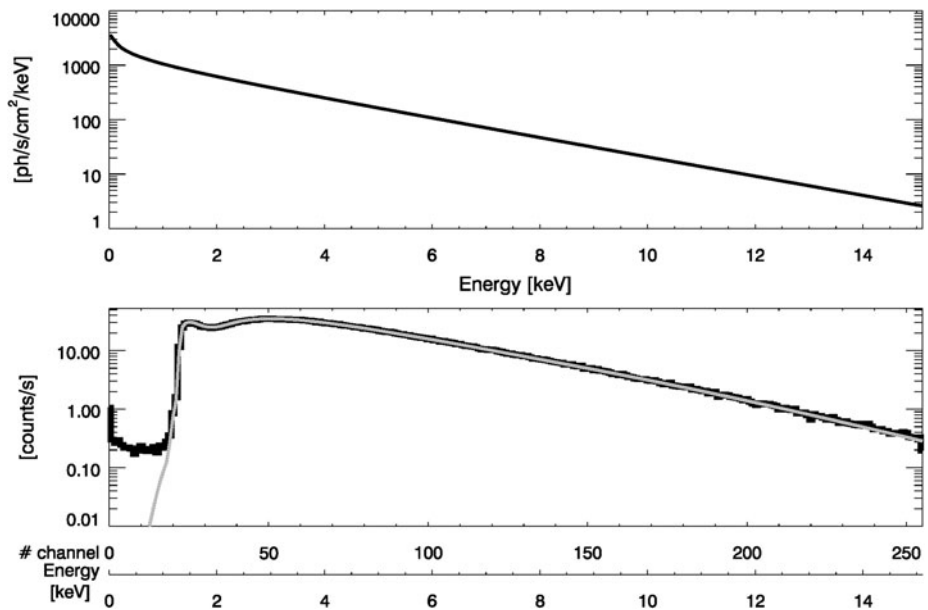


Figure 10 Example of a synchrotron spectrum of undispersed radiation (top). The spectrum from the top panel as measured by SphinX (bottom black line). The spectrum from the top panel folded with the SphinX DRM is overlotted in a gray line.

7. SphinX Scientific Research Areas

Having no spatial resolution, SphinX detectors saw the Sun in the way stars are observed, thus providing measurements of the flux from the entire visible part of the optically thin corona. Hence a comparison of the properties of X-ray emission from the Sun and other

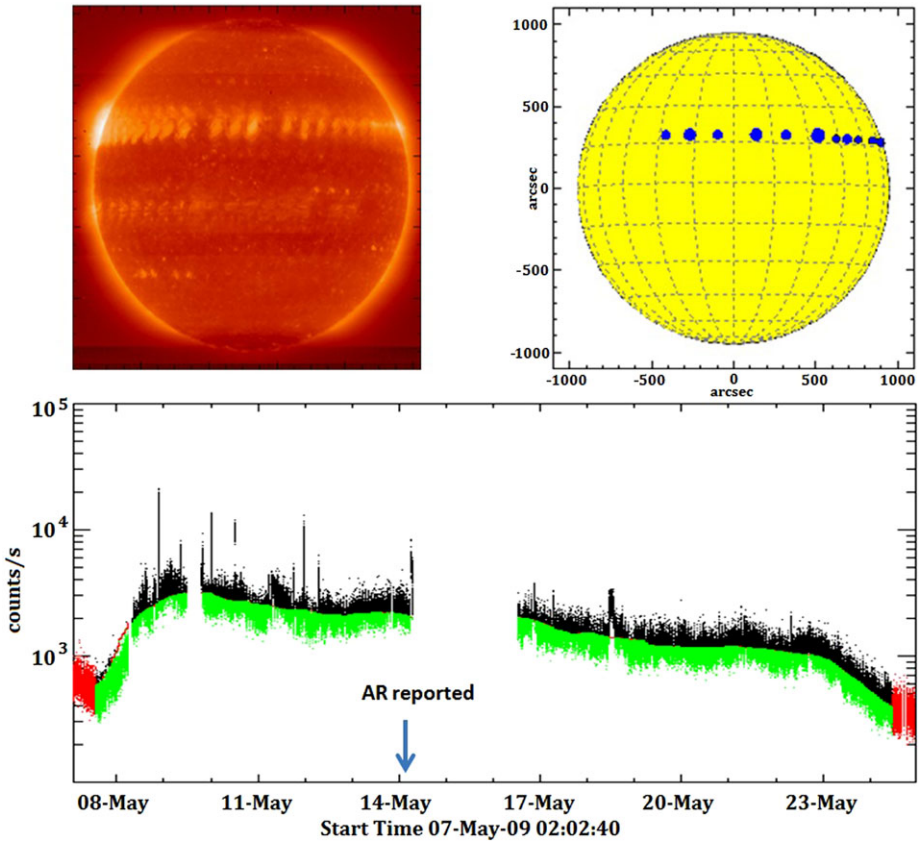


Figure 11 Evolution of Active Region 11017 as seen in SphinX data is shown in the bottom plot. The green line indicates the active-region contribution. The flare component is plotted in black. In the top-left panel a composite image (76 images superimposed) from the XRT telescope is given. It shows that the X-ray emission was dominated by AR 11017 whose path is seen in the northern hemisphere. Some residual X-ray emission was also present in the near equatorial region and southern hemisphere. The top-right panel shows the daily positions of AR 11017 indicated by dark circles. The circle diameter is proportional to the logarithm of the AR area. Positions and sizes were taken from NOAA AR reports. The region was reported with about six days delay from the activity rise observed by SphinX in X-rays.

stars is an interesting research direction, which can be performed with the use of SphinX data. A preliminary comparison of the solar and nearby star X-ray luminosities has already been performed by Sylwester *et al.* (2012) and shows that the Sun was fainter in X-rays than most nearby K and M dwarfs at the time of SphinX operation.

SphinX observed the Sun during extremely low activity, and there are many periods in which it dropped ≈ 20 times below the GOES A1 level. Thus SphinX data open new possibilities in investigations of the quiet Sun. Analysis of SphinX data performed by Sylwester *et al.* (2012) for the 27 most quiet periods revealed an average flux level of $7.21 \pm 1.26 \times 10^{-10} \text{ W m}^{-2}$ in the $1-8 \text{ \AA}$ range, giving a new reference point to the lowest solar-activity level observed in this wavelength range. In these periods usually only a quiet corona with coronal holes and several brightpoints as the only signatures of activity is seen in X-ray images from the XRT (Golub *et al.*, 2007) or TESIS telescopes.

In spite of low solar activity during the entire SphinX mission, substantial flux variability and events typical for higher flux levels were still observed. According to data from NOAA reports, 22 ARs appeared on the visible hemisphere during the SphinX mission. Their reported lifetimes covered a time interval longer than 60 % of the mission duration. SphinX light curves and spectra can be used to determine AR plasma properties and flaring activity, and to trace their evolution on the solar disk. Studies of ARs is another research area that can be performed using SphinX measurements. For some regions such investigations are more straightforward since they travel in isolation, not overlapping the other regions. An example is AR 11017 whose evolution is shown in Figure 11. Another was AR 11024. Preliminary analysis of its properties, flaring activity, and physical parameters such as temperatures, emission measure, and thermodynamic measure in different AR phases can be found in Sylwester *et al.* (2011).

Several hundred small X-ray events have been identified by inspection of SphinX light curves. This small-scale flaring activity was more intense when ARs were present on the visible hemisphere. The strongest one was of GOES class C. The majority of these events have peak intensities below GOES detection threshold. Thus the SphinX team introduced two new intensity classes (S and Q) in order to extend the GOES event classification scale for lower flux values. Class S (for small) covers the flux range 10^{-9} – 10^{-8} W m⁻² and Q (for quiet) the range 10^{-10} – 10^{-9} W m⁻². Some of the events have single-peaked temporal profile with fast rise phase, followed by gradual decay, but most of them are in the form of multi-peaked, complex structures. Analysis of the event properties seen in SphinX data is another field for research. Examples of SphinX observed small flares are shown in Figure 8. A short analysis of their statistical properties can be found in Gburek *et al.* (2011a).

Investigations of SphinX X-ray flux at the time of flares, active regions, and during the presence of coronal holes on the disk give better insight into space weather and climate in a deep activity minimum. Research in this field has direct impact on determining how safe are solar minima periods for piloted or robotic space missions and how to improve the safety of space exploration. Several tens of small flares and brightenings in SphinX dataset were associated in time with CME onsets. Analysis of SphinX data for these events may yield useful information on conditions in solar plasma before CME releases. Flares and CMEs associated with ARs can produce change in solar wind which could be geoeffective even in minimum of activity. Thus ARs need to be monitored in a continuous way.

Reports on solar ARs such as these of NOAA are issued when first sunspots are seen in the photosphere. Hence these reports may come with substantial delay with respect to AR emergence as seen in X-rays. This is shown in Figure 11. AR 11017 was reported with about six days' delay when it had already lost the stronger flaring activity. It is also seen in the SphinX light curve (Figure 2), in the temporal interval between ARs 11014 and 11015 lifetimes, that a longer increase in X-ray flux with more intense flaring, having a temporal profile very similar to ARs, was not reported at all. The above shows that identification, analysis, and monitoring of space-weather events may be improved by using measurements in X-rays from instruments such as SphinX.

Investigation of the particle fluxes recorded by SphinX detectors is also an important field of SphinX data analysis. Such analyses will allow us to characterize the energetic particle environment in the CORONAS-PHOTON orbit and to find out how it evolved during the SphinX mission. Since particles belong to the major threats to humans and instrumentation in space, this activity is also related to space weather, climate, and safety of space exploration.

Studies of SphinX particle observations also are important for the instrument's data interpretation and determining the actual background level which needs to be subtracted from

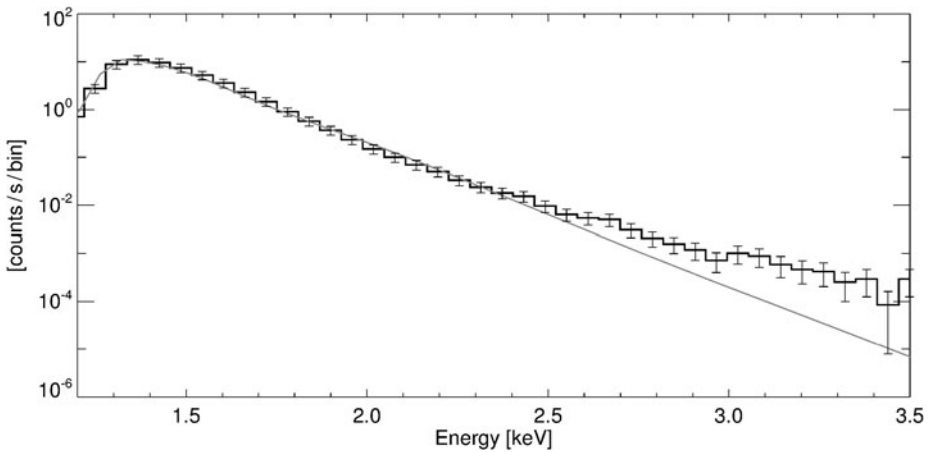


Figure 12 SphinX spectrum of the quiet solar corona (thick histogram). The spectrum was integrated from data recorded on 11 September 2009 between 10:35 and 23:20. The isothermal fit to the spectrum is shown by a thin line.

light curves and spectra during analysis. Some SphinX measurements, particularly those collected in the SAA and radiation belts have very high particle contributions and have to be rejected in analyses focused on solar X-ray fluxes.

Investigations of particle data can also be useful in determining their influence on the detectors and effectiveness of the instrument shielding. This will have impact on the development and constructions of future space-borne instruments.

Spectroscopic analyses of SphinX data allow for determining physical plasma parameters such as temperatures, emission measures, or their distributions. Using SphinX spectra and instrument calibration data one can examine and compare models of ionization equilibria and element abundances used in different spectroscopic analysis packages and databases. An example of a SphinX spectrum of the quiet corona is shown in Figure 12 together with an isothermal fit.

Sylwester *et al.* (2012) analyzed 27 quiet-Sun periods selected in 2009. From this analysis, an average temperature of 1.78 ± 0.07 MK and average logarithm of volume emission measure [cm^{-3}] 47.85 ± 0.14 were obtained for a very quiet corona. It is seen that the isothermal model fits the spectrum well in the lower energy range. Above 2.5 keV there is some excess of the signal over the fit. This is a typical property seen in SphinX spectra. The excess could suggest the existence of a hotter plasma component in a quiet corona. Indeed it was checked that two-component fits with colder component temperature between 1–2 MK and the hotter one ≈ 3 MK could better explain quiet-corona spectra observed by SphinX. The excess over isothermal models is much higher for AR observations. When an AR is present on the disk, a third component with temperatures of ≈ 6 MK is necessary to obtain a good quality fit. Fit models in which differential emission measure (DEM) distributions are used also agree better with the SphinX spectra than isothermal fits. It is, however, uncertain at the moment how much of the signal observed above 2.5 keV comes from background that may be caused by energetic particles as discussed above.

SphinX event-counting observation mode provides an opportunity of waiting-time analysis, investigation of solar-flux changes and fluctuations on very short time scales, and search for non-Maxwellian plasma processes on the Sun.

Comparison of SphinX X-ray and total solar irradiance (TSI) light curves shows that there are some temporal intervals in which increases in SphinX X-ray flux level correlate with increases in TSI. On the other hand, there are periods in which SphinX light curves do not follow the trends observed in the TSI data. These correlations and anti-correlations are particularly well seen during AR presence on the disk.

SphinX data can also be used for cross-calibrations with other X-ray solar instruments such as GOES or RHESSI, for instance. First attempts to compare SphinX and RHESSI spectral observations have already been made (Mrozek *et al.*, 2012). It was found that SphinX data can be used to extend the RHESSI spectra to the low-energy range. Investigations in this area would give the relative sensitivity for the instruments being compared.

8. Conclusions

SphinX data are available from 20 February until 29 November 2009. The data were collected during the deepest-ever solar minimum observed in X-rays. There were no instruments observing at that time with such high energy and temporal resolution and sensitivity covering a similar energy range. Thus SphinX measurements give a reference point – the lowest level of solar activity in X-rays. All SphinX data were reduced to level-1 format ready for scientific analysis. On-line public access to SphinX level-1 has been provided in the form of the internet catalogue. The catalogue also provides calibration information and all documentation necessary for data analysis. The following research areas, in which SphinX measurements may find application, have been identified:

- Analysis of the Sun as a star.
- Investigation of quiet-Sun soft X-ray flux.
- Observations of active regions.
- Identification of small solar events and analysis of their energetics and statistical properties.
- Space weather and climate.
- Characterization of the particle environment in the CORONAS–PHOTON orbit.
- Determination of coronal plasma physical parameters.
- Search for transient and non-Maxwellian processes in solar plasma.
- Comparison of soft X-ray flux and TSI variability.
- Cross-comparison with other X-ray spectrometers.
- Verification of the abundance and ionization equilibrium models used in solar spectroscopy.

The above list is not exhaustive. Soon the activity of the Sun will decrease to a next minimum between Solar Cycles 24 and 25. Activity in this minimum is also expected to be low. Thus another instrument that could provide measurements with SphinX sensitivity or higher would be useful.

Acknowledgements This work obtained support from grant no. N203 381736 of Polish Ministry of Education and Science. SphinX was developed within the framework of the Polish Academy of Sciences and Russian Academy of Sciences bi-lateral agreement on cooperation in space research. The SphinX project was also partially supported by the Russian Foundation for Basic Research (project no. 08-02-01301-a) program for fundamental research of the Physical Department of the Russian Academy of Sciences “Processes in Solar System Plasma”. The research leading to these results has received funding from the European Commission’s Seventh Framework Programme under the grant agreement no. 284461 (eHEROES project). The authors thank the anonymous referee for suggestions and help with preparation of this manuscript.

Appendix: SphinX WWW Resources

XACT facility URL

<http://www.astropa.unipa.it/XACT/>

SphinX level-0 data catalogue in Wroclaw, Poland

http://156.17.94.1/sphinx_catalogue/SphinX_cat_main.html

SphinX level-0 data catalogue in Ondrejow, Czech Republic

http://147.231.104.188/catalog/SphinX_cat_main.html

SphinX level-0 data catalogue in Palermo, Italy

<http://www.sphinx.astropa.unipa.it/>

SphinX level-1 data catalogue in Wroclaw, Poland

http://156.17.94.1/sphinx_l1_catalogue/SphinX_cat_main.html

Description of SphinX level-1 FITS format

http://heasarc.gsfc.nasa.gov/docs/heasarc/ofwg/docs/events/ogip_94_003/ogip_94_003.html

Example of SphinX level-1 FITS file

http://156.17.94.1/sphinx_l1_catalogue/CALIB_SOFT_GUIDE/SPHINX_090704_044307_095331_evn_D1_L1.fits

Description of SphinX response FITS format

ftp://legacy.gsfc.nasa.gov/caldb/docs/memos/cal_gen_92_002/cal_gen_92_002.pdf

SphinX response FITS file

http://156.17.94.1/sphinx_l1_catalogue/CALIB_SOFT_GUIDE/SPHINX_RSP_256_nom_D1.fits

SphinX User Guide

http://156.17.94.1/sphinx_l1_catalogue/CALIB_SOFT_GUIDE/SphinX_user_guide_v1_1.pdf

References

- Bornmann, P.L., Speich, D., Hirman, J., Matheson, L., Grubb, R., Garcia, H., Viereck, R.: 1996, GOES X-ray sensor and its use in predicting solar-terrestrial disturbances. *Proc. SPIE* **2812**, 291–298. ADS:1996SPIE.2812..291B.
- Collura, A., Barbera, M., Varisco, S., Calderone, G., Reale, F., Gburek, S., Kowalinski, M., Sylwester, J., Siarkowski, M., Bakala, J., Podgorski, P., Trzebinski, W., Plocieniak, S., Kordylewski, Z.: 2008, Calibration of the SphinX experiment at the XACT facility in Palermo. *Proc. SPIE* **7011**, 70112U. ADS:2008SPIE.7011E..82C, doi:10.1117/12.789277.
- Gburek, S., Siarkowski, M., Kepa, A., Sylwester, J., Kowalinski, M., Bakala, J., Podgorski, P., Kordylewski, Z., Plocieniak, S., Sylwester, B., Trzebinski, W., Kuzin, S.: 2011a, Soft X-ray variability over the present minimum of solar activity as observed by SphinX. *Solar Syst. Res.* **45**, 182–187. ADS:2011SoSyR..45..182G, doi:10.1134/S0038094611020055.
- Gburek, S., Sylwester, J., Kowalinski, M., Bakala, J., Kordylewski, Z., Podgorski, P., Plocieniak, S., Siarkowski, M., Sylwester, B., Trzebinski, W., Kuzin, S.V., Pertsov, A.A., Kotov, Yu.D., Farnik, F., Reale, F., Phillips, K.J.H.: 2011b, SphinX soft X-ray spectrophotometer: science objectives, design and performance. *Solar Syst. Res.* **45**, 189–199. ADS:2011SoSyR..45..189G, doi:10.1134/S0038094611020067.
- Golub, L., Deluca, E., Austin, G., Bookbinder, J., Caldwell, D., Cheimets, P., Cirtain, J., Cosmo, M., Reid, P., Sette, A., Weber, M., Sakao, T., Kano, R., Shibasaki, K., Hara, H., Tsuneta, S., Kumagai, K., Tamura, T., Shimojo, M., McCracken, J., Carpenter, J., Haight, H., Siler, R., Wright, E., Tucker, J., Rutledge, H., Barbera, M., Peres, G., Varisco, S.: 2007, The X-ray telescope (XRT) for the Hinode mission. *Solar Phys.* **243**, 63–86. ADS:2007SoPh..243..63G, doi:10.1007/s11207-007-0182-1.
- Hanser, F., Sellers, F.: 1996, Design and calibration of the GOES-8 solar X-ray sensor: the XRS. *Proc. SPIE* **2812**, 344–352. ADS:1996SPIE.2812..344H.

- Jain, R., Dave, H., Shah, A.B., Vadher, N.M., Shah, V.M., Ubale, G.P., Manian, K.S., Solanki, B., Chirag, M., Shah, K.J., Kumar, S., Kayasth, S.L., Patel, V.D., Trivedi, J.J., Deshpande, M.R.: 2005, Solar X-ray spectrometer (Soxs) mission on board GSAT2 Indian spacecraft: the low-energy payload. *Solar Phys.* **227**, 89–122. ADS:2005SoPh..227...89J, doi:10.1007/s11207-005-1712-3.
- Klein, R., Thornagel, R., Ulm, G.: 2004, BESSY II Operated as a Primary Source Standard. In: *Proc. EPAC 2004*, 273–275.
- Kotov, Yu.D.: 2011, Scientific goals and observational capabilities of the CORONAS-PHOTON solar satellite project. *Solar Syst. Res.* **45**, 93–96. ADS:2011SoSyR..45...93K, doi:10.1134/S0038094611020079.
- Kuzin, S.V., Zhitnik, I.A., Shestov, S.V., Bogachev, S.A., Bugaenko, O.I., Ignat'ev, A.P., Pertsov, A.A., Ulyanov, A.S., Reva, A.A., Slemzin, V.A., Sukhodrev, N.K., Ivanov, Yu.S., Goncharov, L.A., Mitrofanov, A.V., Popov, S.G., Shergina, T.A., Solov'ev, V.A., Oparin, S.N., Zykov, A.M.: 2011, The TESIS experiment on the CORONAS-PHOTON spacecraft. *Solar Syst. Res.* **45**, 162–173. ADS:2011SoSyR..45..162K, doi:10.1134/S0038094611020110.
- Lin, R.P., Dennis, B.R., Hurford, G.J., Smith, D.M., Zehnder, A., Harvey, P.R., Curtis, D.W., Pankow, D., Turin, P., Bester, M., Csillaghy, A., Lewis, M., Madden, N., van Beek, H.F., Appleby, M., Raudorf, T., McTiernan, J., Ramaty, R., Schmahl, E., Schwartz, R., Krucker, S., Abiad, R., Quinn, T., Berg, P., Hashii, M., Sterling, R., Jackson, R., Pratt, R., Campbell, R.D., Malone, D., Landis, D., Barrington-Leigh, C.P., Slassi-Sennou, S., Cork, C., Clark, D., Amato, D., Orwig, L., Boyle, R., Banks, I.S., Shirey, K., Tolbert, A.K., Zarro, D., Snow, F., Thomsen, K., Henneck, R., McHedlishvili, A., Ming, P., Fivian, M., Jordan, J., Wanner, R., Crubb, J., Preble, J., Matranga, M., Benz, A., Hudson, H., Canfield, R.C., Holman, G.D., Crannell, C., Kosugi, T., Emslie, A.G., Vilmer, N., Brown, J.C., Johns-Krull, C., Aschwanden, M., Metcalf, T., Conway, A.: 2002, The Reuven Ramaty High-Energy Solar Spectroscopic Imager (RHESSI). *Solar Phys.* **210**, 3–32. ADS:2002SoPh..210....3L, doi:10.1023/A:1022428818870.
- Mrozek, T., Gburek, S., Siarkowski, M., Sylwester, B., Sylwester, J., Gryciuk, M.: 2012, Common SphinX and RHESSI observations of solar flares. *Cent. Eur. Astrophys. Bull.* **36**, 71–82. ADS:2012CEAB...36...71M.
- Reinard, A., Hill, S., Viereck, R., Bailey, S.: 2005, Calibration of GOES/SXI and XRS instruments. In: *AGU, Fall Meeting 2005*, abstract #SH23B-0344, ADS:2005AGUFMESH23B0344R.
- Sylwester, J., Kuzin, S., Kotov, Yu.D., Farnik, F., Reale, F.: 2008, SphinX: a fast solar photometer in X-rays. *J. Astrophys. Astron.* **29**, 339–343. ADS:2008JApA...29..339S, doi:10.1007/s12036-008-0044-8.
- Sylwester, B., Sylwester, J., Siarkowski, M., Engell, A.J., Kuzin, S.V.: 2011, Physical characteristics of AR 11024 plasma based on SPHINX and XRT data. *Cent. Eur. Astrophys. Bull.* **35**, 171–180. ADS:2011CEAB...35..171S.
- Sylwester, J., Kowalinski, M., Gburek, S., Siarkowski, M., Kuzin, S., Farnik, F., Reale, F., Phillips, K.J.H., Bakala, J., Gryciuk, M., Podgorski, P., Sylwester, B.: 2012, SphinX measurements of the 2009 solar minimum X-ray emission. *Astrophys. J.* **751**, 111. ADS:2012ApJ...751..111S, doi:10.1088/0004-637X/751/2/111.